# VIBRATIONAL RESPONSE OF SYMMETRICALLY LAMINATED TRAPEZOIDAL COMPOSITE PLATES WITH POINT CONSTRAINTS

## K. M. LIEW

School of Mechanical and Production Engineering, Nanyang Technological University,
Nanyang Avenue, Singapore 2263

and

## K. Y. LAM

Department of Mechanical and Production Engineering, National University of Singapore,
10 Kent Ridge Crescent, Singapore 0511

Abstract—This paper presents the first known results for free vibrations of thin, points-supported, symetrically laminated trapezoidal composite plates. The solution method developed is based on the Rayleigh–Ritz method and the admissible 2-D orthogonal polynomials to derive the governing eigenvalue equation. The natural frequencies and mode shapes for the laminated plates are obtained by solving this governing eigenvalue equation. Several test problems are solved to demonstrate the accuracy and flexibility of the proposed method. The effects of fibre orientations, points location and the number of layers in the stacking sequences on the vibrational response for the plate problems are investigated. Variation of spring constants for the elastic points on the effect of the frequency parameters is also considered.

## NOTATION

| | |
|---|---|
| $a,b$ | sides of plate |
| $C_q$ | coefficients |
| $[D]$ | bending stiffness coefficients |
| $D_0$ | $E_1 h^3/12(1-v_{12}v_{21})$ |
| $E_1, E_2$ | Young's moduli parallel to and perpendicular to fibres |
| $g_m(\xi, \eta)$ | generating function |
| $h$ | plate thickness |
| $[K]$ | bending curvatures |
| $[M]$ | moment resultants |
| $R$ | plate domain |
| $T_{max}$ | maximum kinetic energy |
| $V_{max}$ | maximum strain energy |
| $W(\xi, \eta)$ | displacement function |
| $x, y$ | Cartesian coordinates |
| $\alpha$ | plate aspect ratio $(a/b)$ |
| $\beta$ | fibre orientation angle |
| $\Phi_i(\xi, \eta)$ | 2-D orthogonal polynomial function |
| $\eta$ | $y/b$ |
| $\psi_{m,n}$ | constants (coefficients) |
| $\lambda$ | frequency parameter $(\rho h \omega^2 a^4/D_0)$ |
| $\rho$ | density per unit area of plate |
| $v_{12}, v_{21}$ | Poisson's ratios |
| $\omega$ | radian frequency |
| $\xi$ | $x/a$ |
| $\lceil x \rceil$ | greatest integer function |

## 1. INTRODUCTION

In the open literature, rather few publications are available for vibration analysis of thin symmetrically laminated quadrilateral plates except for the rectangular plates (Ashton and Anderson, 1969; Whitney, 1971; Mohan and Kingsbury, 1971). As we know, the analysis is considerably complicated and exact solutions are out of the question, therefore approximate methods are employed for the solutions of these plate problems. A brief review for the reactangular plate problems has been given by Leissa and Narita (1989).

For plates other than rectangular shape, two papers are available. The vibration analysis of single-layer composite skew plates was first studied by Nair and Durvasula (1974). The formulation is based on orthotropic plate theory with arbitrary orientation of the principal axes of orthotropy. Approximate solutions for the frequencies and mode shapes were obtained by the Rayleigh–Ritz method using the products of appropriate beam characteristic functions as the admissible functions. The variation of frequencies and mode shapes with orientation of the axes of orthotropy was examined for different skew angles and boundary conditions. The second available paper was published by Srinivasam and Ramachandran (1975). They presented a numerical method for finding the natural frequencies and mode shapes of single-layer parallel fibre fully clamped skew plates with or without being subjected to in-plane forces. The numerical method employed makes use of integral equations of beams with appropriate boundary conditions along the skew co-ordinates for transforming the governing differential equation into a set of algebraic equations. Natural frequencies and mode shapes for several fully clamped skew plates having different orientations of the axes of orthotropy were obtained by solving these equations.

The present paper presents a general numerical method to study the transverse vibration of symmetrically laminated trapezoidal plates with point constraints. The method has been used in previous papers to study the vibration of isotropic and anisotropic trapezoidal plates (Liew and Lam, 1990, 1991a,b). The analysis involves using a set of 2-D orthogonal polynomials as the admissible displacement function in the Rayleigh–Ritz method to derive the governing eigenvalue equation. In this paper, the set of 2-D orthogonal polynomials is further extended to study the aforementioned plate problems. The aim of this paper is to provide a set of accurate results for the free vibration frequencies of these symmetrically laminated points supported trapezoidal composite plates for which no exact solutions are possible. Mode shapes for several laminated composite plates are presented by means of contour plots.

## 2. PROBLEM DEFINITION

Consider a thin, fibre-reinforced composite, laminated trapezoidal plate continuous over point supports, lying in the $x$–$y$ plane, and bounded by $-a/2 \leqslant x \leqslant a/2$ and $-b/2 \leqslant y \leqslant b/2$, as shown in Fig. 1. The plate, with thickness $h$ in the $z$-direction, consists of $n$ layers of orthotropic plies perfectly bonded together by a matrix material. The reference plane $z = 0$ is considered to be located at the undeformed middle plane as shown in Fig. 2. The fibre direction within a layer is indicated by the angle $\beta$. The moduli of elasticity for a layer parallel to the fibres is $E_1$ and perpendicular to the fibres is $E_2$.

## 3. METHOD OF SOLUTION

In the present study, the layers are so arranged that a mid-plane symmetry exists. By these special symmetrical arrangements, coupling between transverse bending and in-plane stretching is solved. An attempt is made to solve the natural frequencies and mode shapes
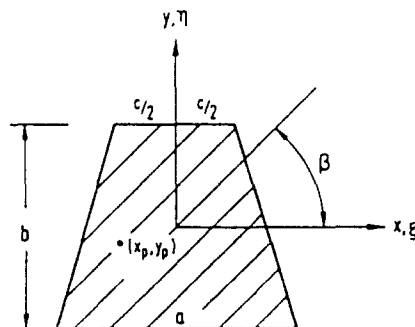


Fig. 1. Geometry of a trapezoidal plate with fibre direction $\beta$ having point support located at $(x_p, y_p)$.
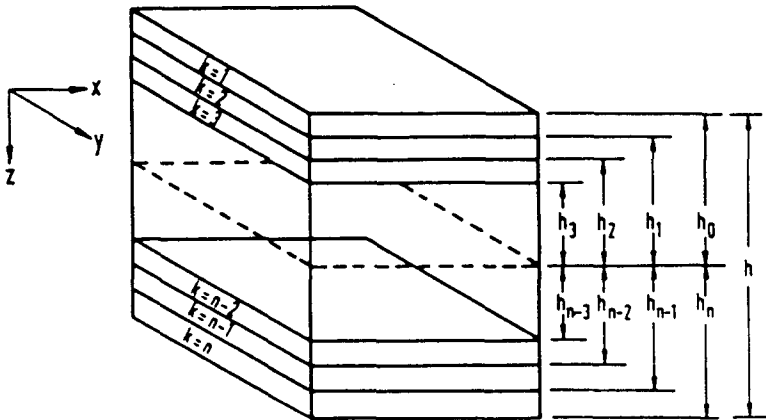
Fig. 2. Layer co-ordinates and orientation for laminates.

of these problems approximately by using the Rayleigh–Ritz approach with a set of 2-D orthogonal polynomials.

The strain energy due to bending can be expressed as

$$V_{max} = \frac{1}{2}\int\int_R [M][K]\,dx\,dy \qquad (1)$$

where the integration is carried out over the entire plate domain $R$ and

$$[M] = [M_x, M_y, M_{xy}]^t \qquad (2)$$

$$[K] = [K_x, K_y, K_{xy}] \qquad (3)$$

in which [M] is moment resultant and [K] is bending curvature.

The bending curvatures are related to the displacements by

$$K_x = \frac{\partial^2 W}{\partial x^2} \qquad (4)$$

$$K_y = \frac{\partial^2 W}{\partial y^2} \qquad (5)$$

$$K_{xy} = 2\frac{\partial^2 W}{\partial x\,\partial y}. \qquad (6)$$

For anisotropic materials, the moment resultants are given by

$$[M] = [D][K] \qquad (7)$$

where [D] is a 3 × 3 symmetric matrix of bending stiffness coefficients.

For symmetric angle-ply laminates, the coefficients of the bending stiffness matrix are given by

$$D_{ct} = \frac{1}{3}\sum_{k=1}^{m} (N_{ct})_k (h_k^3 - h_{k-1}^3); \ c,t = 1,2,6. \qquad (8)$$

$(N_{ct})_k$ are the reduced stiffness of the $k$th ply which are defined by the elastic constants of the layer and fibre orientation angle $\beta_k$. $(N_{ct})_k$ are given by

$$N_{11_k} = Q_{11_k} \cos^4 \beta_k + 2(Q_{12_k} + 2Q_{66_k}) \sin^2 \beta_k \cos^2 \beta_k + Q_{22_k} \sin^4 \beta_k \tag{9}$$

$$N_{12_k} = (Q_{11_k} + Q_{22_k} - 4Q_{66_k}) \sin^2 \beta_k \cos^2 \beta_k + Q_{12_k}(\sin^4 \beta_k + \cos^4 \beta_k) \tag{10}$$

$$N_{22_k} = Q_{11_k} \sin^4 \beta_k + 2(Q_{12_k} + 2Q_{66_k}) \sin^2 \beta_k \cos^2 \beta_k + Q_{22_k} \cos^4 \beta_k \tag{11}$$

$$N_{16_k} = (Q_{11_k} - Q_{12_k} - Q_{66_k}) \sin \beta_k \cos^3 \beta_k + (Q_{12_k} - Q_{22_k} + 2Q_{66_k}) \sin^3 \beta_k \cos \beta_k \tag{12}$$

$$N_{26_k} = (Q_{11_k} - Q_{12_k} - 2Q_{66_k}) \sin^3 \beta_k \cos \beta_k + (Q_{12_k} - Q_{22_k} + 2Q_{66_k}) \sin \beta_k \cos^3 \beta_k \tag{13}$$

$$N_{66_k} = (Q_{11_k} + Q_{22_k} - 2Q_{12_k} - 2Q_{66_k}) \sin^2 \beta_k \cos^2 \beta_k + Q_{66_k}(\sin^4 \beta_k + \cos^4 \beta_k) \tag{14}$$

where

$$Q_{11_k} = \frac{E_{1_k}}{1 - \nu_{12_k} \nu_{21_k}} \tag{15}$$

$$Q_{12_k} = \frac{\nu_{12_k} E_{2_k}}{1 - \nu_{12_k} \nu_{21_k}} \tag{16}$$

$$Q_{22_k} = \frac{E_{2_k}}{1 - \nu_{12_k} \nu_{21_k}} \tag{17}$$

$$Q_{66_k} = G_{12_k} \tag{18}$$

$$\nu_{21_k} E_{1_k} = \nu_{12_k} E_{2_k} \tag{19}$$

in which $E_{1_k}$ and $E_{2_k}$ are the Young's moduli parallel to and perpendicular to the fibres and $\nu_{12_k}$ and $\nu_{21_k}$ are the corresponding Poisson's ratios.

Substituting eqns (2)–(8) into eqn (1) results in

$$V_{max} = \frac{1}{2} \iint_R \left\{ D_{11} \left[ \frac{\partial^2 W}{\partial x^2} \right]^2 + 2D_{12} \left[ \frac{\partial^2 W}{\partial x^2} \frac{\partial^2 W}{\partial y^2} \right] + D_{22} \left[ \frac{\partial^2 W}{\partial y^2} \right]^2 + 4D_{16} \left[ \frac{\partial^2 W}{\partial x^2} \frac{\partial^2 W}{\partial x \partial y} \right] \right.$$
$$\left. + 4D_{26} \left[ \frac{\partial^2 W}{\partial y^2} \frac{\partial^2 W}{\partial x \partial y} \right] + 4D_{66} \left[ \frac{\partial^2 W}{\partial x \partial y} \right]^2 \right\} dx \, dy. \tag{20}$$

If a plate with elastic point supports is considered, additional strain energy stored in the vertical deflection springs exists. This additional strain energy is given by

$$V_2 = \frac{\Omega}{2} \sum_{r=1}^{p} [W(x_r, y_r)]^2 \tag{21}$$

where $(x_r, y_r)$ are the locations of elastic point supports and $p$ is the number of elastic point constraints.

The total maximum strain energy is obtained by summing the contributions from eqns (20) and (21) resulting in

$$V_{max} = V_1 + V_2. \tag{22}$$

The maximum kinetic energy of the plate during small amplitude vibration is given by

$$T_{max} = \tfrac{1}{2}\rho h\omega^2 \iint_R W^2(x, y)\,dx\,dy \qquad (23)$$

where $\rho$ is the mass per unit area of plate, $h$ is the thickness and $\omega$ is the angular frequency of vibration.

The displacement function $W(\xi, \eta)$ may be expressed in terms of 2-D orthogonal polynomials which is given by

$$W(\xi, \eta) = \sum_{q=1}^{n} C_q \Phi_q(\xi, \eta) \qquad (24)$$

where $\xi = x/a$, $\eta = y/b$ and $C_q$ are the unknown coefficients.

Substituting eqn (24) into eqns (22) and (23) results in

$$
V_{max} = \frac{1}{2}\iint_R \left\{ \frac{D_{11}}{a^4}\left[\frac{\partial^2 \sum_{q=1}^{n} C_q \Phi_q(\xi, \eta)}{\partial \xi^2}\right]^2 \right.
$$

$$
+ \frac{2D_{12}}{a^2 b^2}\left[\frac{\partial^2 \sum_{q=1}^{n} C_q \Phi_q(\xi, \eta)}{\partial \xi^2}\frac{\partial^2 \sum_{q=1}^{n} C_q \Phi_q(\xi, \eta)}{\partial \eta^2}\right] + \frac{D_{22}}{b^4}\left[\frac{\partial^2 \sum_{q=1}^{n} C_q \Phi_q(\xi, \eta)}{\partial \eta^2}\right]^2
$$

$$
+ \frac{4D_{16}}{a^3 b}\left[\frac{\partial^2 \sum_{q=1}^{n} C_q \Phi_q(\xi, \eta)}{\partial \xi^2}\frac{\partial^2 \sum_{q=1}^{n} C_q \Phi_q(\xi, \eta)}{\partial \xi \partial \eta}\right]
$$

$$
+ \frac{4D_{26}}{ab^3}\left[\frac{\partial^2 \sum_{q=1}^{n} C_q \Phi_q(\xi, \eta)}{\partial \eta^2}\frac{\partial^2 \sum_{q=1}^{n} C_q \Phi_q(\xi, \eta)}{\partial \xi \partial \eta}\right]
$$

$$
\left. + \frac{4D_{66}}{a^2 b^2}\left[\frac{\partial^2 \sum_{q=1}^{n} C_q \Phi_q(\xi, \eta)}{\partial \xi \partial \eta}\right]^2 \right\}\,d\xi\,d\eta + \frac{\Omega}{2}\sum_{r=1}^{p}\sum_{q=1}^{n}[C_q \Phi_q(\xi_r, \eta_r)]^2 \qquad (25)
$$

$$T_{max} = \frac{\rho h\omega^2}{2}\iint_R \sum_{q=1}^{n}[C_q \Phi_q(\xi, \eta)]^2\,d\xi\,d\eta. \qquad (26)$$

By minimizing the energy functional $(V_{max} - T_{max})$ with respect to each coefficient $C_q$

$$\frac{\partial}{\partial C_q}(V_{max} - T_{max}) = 0, \quad q = 1, 2, \ldots, n \qquad (27)$$

leads to the governing eigenvalue equation

$$\sum (K_{ij} + S_i L_{ij} - \lambda M_{ij})C_i = 0, \quad i,j = 1, 2, \ldots, n \qquad (28)$$

where the parameters $S_i$ and $\lambda$ are given by

$$S_i = \frac{\Omega a^4}{D_0} \qquad (29)$$

$$\lambda = \frac{\rho h\omega^2 a^4}{D_0} \qquad (30)$$

$$D_0 = \frac{E_1 h^3}{12(1 - v_{12} v_{21})} \tag{31}$$

in which

$$K_{ij} = \frac{1}{D_0} \{ D_{11}(F_{ij})_1 + \alpha^4 D_{22}(F_{ij})_2 + \alpha^2 D_{12}[(F_{ij})_3 + (F_{ij})_4] + 2\alpha D_{16}[(F_{ij})_5 + (F_{ij})_6]$$
$$+ 2\alpha^3 D_{26}[(F_{ij})_7 + (F_{ij})_8] + 4\alpha^2 D_{66}(F_{ij})_9 \} \tag{32}$$

$$L_{ij} = \sum_{r=1}^{p} \Phi_i(\xi_r, \eta_r)\Phi_j(\xi_r, \eta_r) \tag{33}$$

$$M_{ij} = \iint_R \Phi_i(\xi, \eta)\Phi_j(\xi, \eta) \, d\xi \, d\eta. \tag{34}$$

$[K]$ and $[L]$ are symmetrical matrices, and $[M]$ is a diagonal matrix. Equation (28) forms a set of $i \times j$ homogeneous linear simultaneous equations expressed in terms of the unknown coefficients $C_i$. For a non-trivial solution, the determinant of the coefficient matrix is set to zero. There are $i \times j$ values of $\lambda$ that satisfy eqn (28), which are each upper-bound approximations to the exact frequencies.

Several terms on the right-hand side of eqn (32) need to be defined; these are

$$\alpha = \frac{a}{b} \tag{35}$$

$$(F_{ij})_1 = \iint_R \left[ \frac{\partial^2 \Phi_i(\xi, \eta)}{\partial \xi^2} \right]\left[ \frac{\partial^2 \Phi_j(\xi, \eta)}{\partial \xi^2} \right] d\xi \, d\eta \tag{36}$$

$$(F_{ij})_2 = \iint_R \left[ \frac{\partial^2 \Phi_i(\xi, \eta)}{\partial \eta^2} \right]\left[ \frac{\partial^2 \Phi_j(\xi, \eta)}{\partial \eta^2} \right] d\xi \, d\eta \tag{37}$$

$$(F_{ij})_3 = \iint_R \left[ \frac{\partial^2 \Phi_i(\xi, \eta)}{\partial \eta^2} \right]\left[ \frac{\partial^2 \Phi_j(\xi, \eta)}{\partial \xi^2} \right] d\xi \, d\eta \tag{38}$$

$$(F_{ij})_4 = \iint_R \left[ \frac{\partial^2 \Phi_i(\xi, \eta)}{\partial \xi^2} \right]\left[ \frac{\partial^2 \Phi_j(\xi, \eta)}{\partial \eta^2} \right] d\xi \, d\eta \tag{39}$$

$$(F_{ij})_5 = \iint_R \left[ \frac{\partial^2 \Phi_i(\xi, \eta)}{\partial \xi^2} \right]\left[ \frac{\partial^2 \Phi_j(\xi, \eta)}{\partial \xi \, \partial \eta} \right] d\xi \, d\eta \tag{40}$$

$$(F_{ij})_6 = \iint_R \left[ \frac{\partial^2 \Phi_i(\xi, \eta)}{\partial \xi \, \partial \eta} \right]\left[ \frac{\partial^2 \Phi_j(\xi, \eta)}{\partial \xi^2} \right] d\xi \, d\eta \tag{41}$$

$$(F_{ij})_7 = \iint_R \left[ \frac{\partial^2 \Phi_i(\xi, \eta)}{\partial \eta^2} \right]\left[ \frac{\partial^2 \Phi_j(\xi, \eta)}{\partial \xi \, \partial \eta} \right] d\xi \, d\eta \tag{42}$$

$$(F_{ij})_8 = \iint_R \left[ \frac{\partial^2 \Phi_i(\xi, \eta)}{\partial \xi \, \partial \eta} \right]\left[ \frac{\partial^2 \Phi_j(\xi, \eta)}{\partial \eta^2} \right] d\xi \, d\eta \tag{43}$$

$$(F_{ij})_9 = \int\int_R \left[ \frac{\partial^2 \Phi_i(\xi, \eta)}{\partial \xi \, \partial \eta} \right] \left[ \frac{\partial^2 \Phi_j(\xi, \eta)}{\partial \xi \, \partial \eta} \right] d\xi \, d\eta. \tag{44}$$

### 4. ADMISSIBLE DISPLACEMENT FUNCTIONS

The displacement function $W(\xi, \eta)$ as given in eqn (24), is expressed in terms of a series of 2-D orthogonal polynomials. The recurrence formula for 2-D orthogonal polynomials involves every other member in the set

$$\Phi_m(\xi, \eta) = g_m(\xi, \eta)\Phi_1(\xi, \eta) - \sum_{n=1}^{m-1} \psi_{m,n}\Phi_n(\xi, \eta); \quad m > 1 \tag{45}$$

where $\psi_{m,n}$ is a constant and $g_m(\xi, \eta)$ is a generating function. The constant $\psi_{m,n}$ is given by

$$\psi_{m,n} = \frac{\int\int_R g_m(\xi, \eta)\Phi_1(\xi, \eta)\Phi_n(\xi, \eta) \, d\xi \, d\eta}{\int\int_R \Phi_n^2(\xi, \eta) \, d\xi \, d\eta}. \tag{46}$$

By using this recurrence formula, the inner product of any two different members in the series satisfies the orthogonality condition

$$\int\int_R \Phi_m(\xi, \eta)\Phi_n(\xi, \eta) \, d\xi \, d\eta = \begin{cases} 0 & \text{if} \quad m \neq n \\ 1 & \text{if} \quad m = n \end{cases}. \tag{47}$$

*(i) Generating functions*

The generating function $g_m(\xi, \eta)$ which are obtained empirically can be determined by the following general procedures.

The parameters $\alpha_1$ and $\alpha_2$ are determined from the expressions

$$\alpha_1 = \lceil \sqrt{m-1} \rceil \tag{48}$$

$$\alpha_2 = (m-1) - \alpha_1^2. \tag{49}$$

If $\alpha_1$ is an even number then the generating function is given by

$$g_m(\xi, \eta) = \xi^{\alpha_1}\eta^{\alpha_3} \tag{50}$$

where $\alpha_3$ is defined as

$$\alpha_3 = \frac{\alpha_2}{2}; \quad 0 \leqslant \alpha_3 \leqslant \alpha_1. \tag{51}$$

On the other hand, if $\alpha_1$ is an odd number then the generating function becomes

$$g_m(\xi, \eta) = \xi^{\alpha_1}\eta^{\alpha_3} \tag{52}$$

where $\alpha_3$ now is defined as

$$\alpha_3 = \frac{(\alpha_2 - 1)}{2}; \quad 1 \leqslant \alpha_3 \leqslant \alpha_1. \tag{53}$$

The symbol $\lceil \quad \rceil$ adopted in eqn (48) denotes the greatest integer function.

*(ii) Determination of starting functions*

The starting functions $\Phi_1(\xi, \eta)$ chosen for the analysis must satisfy the prescribed boundary conditions of the plate. In the present study, the starting functions are constructed to satisfy the geometrical boundary conditions since they are the only necessary requirement for the admissible functions in the Rayleigh–Ritz method. The geometrical boundary conditions are $\Phi_1 = 0$ for simply supported edges, $\Phi_1 = \partial\Phi_1/\partial n = 0$ for clamped edges and no geometrical boundary condition exists for free edges.

For trapezoidal plate, the starting function is given by

$$\Phi_1(\xi, \eta) = \prod_{i=1}^{4} \chi_i(\xi, \eta) \tag{54}$$

where $\chi_i(\xi, \eta)$ are the edge functions.

By applying the appropriate boundary conditions, the edge functions for the edges can be obtained. For the simply supported edges, the edge functions are given by

$$\chi_i(\xi, \eta) = \begin{cases} \xi - a & \text{for edges } \xi = a \\ \eta - b & \text{for edges } \eta = b \\ \eta - \bar{m}\xi - c & \text{for edges } \eta = \bar{m}\xi + c \end{cases} \tag{55}$$

and the edge functions for the clamped edges are given by

$$\chi_i(\xi, \eta) = \begin{cases} (\xi - a)^2 & \text{for edges } \xi = a \\ (\eta - b)^2 & \text{for edges } \eta = b \\ (\eta - \bar{m}\xi - c)^2 & \text{for edges } \eta = \bar{m}\xi + c \end{cases} \tag{56}$$

and the edge functions for the free edges are given by

$$\chi_i(\xi, \eta) = 1. \tag{57}$$

## 5. NUMERICAL EXAMPLES

As we know, variation in ply orientation will alter the characteristic sitffness of plates. To demonstrate this behaviour, several plates are studied. In this paper, the eigenvalues obtained are expressed in terms of non-dimensional frequency parameters $(\rho h \omega^2 a^4 / D_0)^{1/2}$. The material used in the present analysis is the graphite/epoxy composite and the properties are given in Table 1.

### 5.1. Centrally-located point supports

The first set of problems treated is that of laminated cantilevered trapezoidal plates $(a/b = 1)$ having the edge clamped at $y = b/2$. The plates are supported by an elastic point located at the centre $(x = 0, y = 0)$.

The first example considered is an eight-ply laminated trapezoidal plate with the stacking sequence of $[(0, 90, 90, 0)]_{\text{sym}}$ having various values of the $c/a$ ratio. Convergence study is carried out for the plate having ratios $a/b = 1$ and $c/a = 2/5$. The convergence

Table 1. Material properties of unidirectional composite

| Material | $E_1$ (GPa) | $E_2$ (GPa) | $G_{12}$ (GPa) | $v_{12}$ |
| --- | --- | --- | --- | --- |
| G/E | 138 | 8.96 | 7.1 | 0.30 |

Table 2. Convergence patterns of frequency parameters $(\rho h \omega^2 a^4 D_n)^{1/2}$ for an eight-layer laminated centrally elastic point supported cantilevered trapezoidal plate $(a/b = 1,\ c/a = 2/5)$ having a stacked sequence of $[(0,90,90,0)]_{sym}$

| $S_r$ | Terms | Mode sequence number | | | | | |
|---|---|---|---|---|---|---|---|
| | | 1 | 2 | 3 | 4 | 5 | 6 |
| 100 | 36 | 8.32 | 8.68 | 26.58 | 27.53 | 48.81 | 56.34 |
| | 40 | 8.23 | 8.68 | 26.58 | 26.88 | 48.70 | 56.33 |
| | 46 | 8.19 | 8.67 | 26.58 | 26.77 | 48.65 | 56.33 |
| | 50 | 8.19 | 8.67 | 26.58 | 26.76 | 48.65 | 56.33 |
| $\infty$ | 36 | 8.63 | 8.68 | 26.58 | 28.70 | 48.93 | 56.34 |
| | 40 | 8.53 | 8.68 | 26.58 | 27.95 | 48.83 | 56.33 |
| | 46 | 8.50 | 8.67 | 26.58 | 27.82 | 48.80 | 56.33 |
| | 50 | 8.49 | 8.67 | 26.58 | 27.81 | 48.79 | 56.33 |

Table 3. Frequency parameters $(\rho h \omega^2 a^4 D_n)^{1/2}$ of an eight-layer laminated centrally elastic point supported cantilevered trapezoidal plate $(a/b = 1)$ with a stacking sequence of $[(0,90,90,0)]_{sym}$

| $c/a$ | $S_r$ | Mode sequence number | | | | | |
|---|---|---|---|---|---|---|---|
| | | 1 | 2 | 3 | 4 | 5 | 6 |
| 2/5 | 1 | 4.21 | 8.67 | 18.88 | 26.58 | 38.64 | 49.18 |
| | 10 | 6.52 | 8.67 | 21.96 | 26.58 | 41.97 | 49.34 |
| | 100 | 8.19 | 8.67 | 26.58 | 26.76 | 48.65 | 56.33 |
| | 1000 | 8.46 | 8.67 | 26.58 | 27.70 | 48.78 | 56.33 |
| | 10000 | 8.49 | 8.67 | 26.58 | 27.80 | 48.79 | 56.33 |
| | $\infty$ | 8.49 | 8.67 | 26.58 | 27.81 | 48.79 | 56.33 |
| 4/5 | 1 | 3.45 | 5.18 | 17.91 | 20.94 | 22.66 | 34.16 |
| | 10 | 5.18 | 5.18 | 19.11 | 20.94 | 25.55 | 36.41 |
| | 100 | 5.18 | 6.45 | 19.71 | 20.94 | 29.51 | 48.74 |
| | 1000 | 5.18 | 6.67 | 19.79 | 20.94 | 29.99 | 48.87 |
| | 10000 | 5.18 | 6.69 | 19.79 | 20.94 | 30.03 | 48.88 |
| | $\infty$ | 5.18 | 6.69 | 19.79 | 20.94 | 30.04 | 48.88 |

patterns obtained for the plate are given in Table 2. It can be seen that 50 terms are required to obtain the convergent results. The effect of spring constants upon the frequency parameters of the plate is studied and the results are given in Table 3. Displacement contour plots to represent the mode shapes of the plates with a centrally located rigid point support having various $c/a$ ratios are presented in Fig. 3.



$\sqrt{\lambda_1} = 8.49$  $\sqrt{\lambda_2} = 8.67$  $\sqrt{\lambda_3} = 26.58$  $\sqrt{\lambda_4} = 27.81$  $\sqrt{\lambda_5} = 48.79$  $\sqrt{\lambda_6} = 56.33$

(a) c/a = 2/5

$\sqrt{\lambda_1} = 5.18$  $\sqrt{\lambda_2} = 6.69$  $\sqrt{\lambda_3} = 19.79$  $\sqrt{\lambda_4} = 20.94$  $\sqrt{\lambda_5} = 30.04$  $\sqrt{\lambda_6} = 48.88$
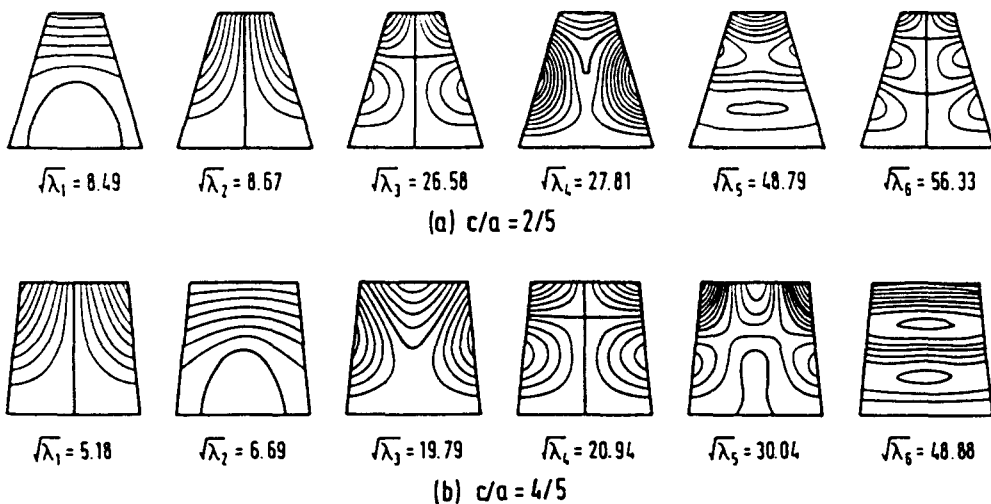
(b) c/a = 4/5

Fig. 3. Contour plots for the mode shapes of the eight-layer G/E centrally point supported trapezoidal plates $(a/b = 1)$ with stacking sequence of $[0,90,90,0]_{sym}$.

Table 4. Frequency parameters $(\rho\omega^2 a^4/D_0)^{1/2}$ of a sixteen-layer laminated centrally elastic point supported cantilevered trapezoidal plate $(a/b = 1)$ with a stacking sequence of $[(0,45,-45,90)_2]_{sym}$

| | | Mode sequence number | | | | | |
|---|---|---|---|---|---|---|---|
| $c/a$ | $S$ | 1 | 2 | 3 | 4 | 5 | 6 |
| 2/5 | 1 | 3.97 | 11.24 | 17.71 | 31.45 | 45.49 | 45.74 |
| | 10 | 6.36 | 11.26 | 20.70 | 31.46 | 45.74 | 47.94 |
| | 100 | 8.31 | 11.28 | 28.35 | 31.55 | 45.74 | 61.25 |
| | 1000 | 8.63 | 11.28 | 30.41 | 31.78 | 45.74 | 61.29 |
| | 10000 | 8.67 | 11.28 | 30.59 | 31.85 | 45.74 | 61.30 |
| | $\infty$ | 8.67 | 11.28 | 30.61 | 31.86 | 45.74 | 61.30 |
| 4/5 | 1 | 3.28 | 6.98 | 16.77 | 23.65 | 25.25 | 46.15 |
| | 10 | 5.21 | 6.99 | 18.62 | 23.78 | 26.97 | 46.21 |
| | 100 | 6.81 | 7.20 | 20.92 | 23.90 | 37.96 | 46.60 |
| | 1000 | 6.90 | 7.45 | 21.24 | 23.92 | 42.50 | 47.10 |
| | 10000 | 6.90 | 7.48 | 21.28 | 23.92 | 42.91 | 47.19 |
| | $\infty$ | 6.90 | 7.49 | 21.28 | 23.92 | 42.95 | 45.21 |

The second example considered is a sixteen-ply laminated trapezoidal plate with stacking sequence of $[(0,45,-45,90)_2]_{sym}$. The effect on the vibrational response by increasing the spring constants is investigated for the plate with $c/a = 2/5$ and $4/5$. The results obtained using 50 terms for the plate having various values of spring constants and $c/a$ ratios are given in Table 4. The first six mode shapes for the plate are also obtained and presented in Fig. 4 together with the corresponding frequency parameters given below each mode. The mode shapes shown in Fig. 4 are obtained for the plate having a centrally located rigid point support.

5.2. *Point supports located on the edge*

The second set of problems treated is that of laminated cantilevered trapezoidal plates $(a/b = 1)$ with the clamped edge at $y = -b/2$ having point supports located at the opposite corners of the clamped edge. Vibration analysis is carried out for these plates having $c/a = 2/5$ and $4/5$ and the results for different ply oriented laminates are presented. The point supports for the laminated trapezoidal plates located: (a) for $c/a = 2/5$ at $x = -a/5$, $y = a/2$ and at $x = a/5$, $y = a/2$, and (b) for $c/a = 4/5$ at $x = -2a/5$, $y = a/2$ and at $x = 2a/5$, $y = a/2$.



$\sqrt{\lambda_1} = 8.67$    $\sqrt{\lambda_2} = 11.28$    $\sqrt{\lambda_3} = 30.61$    $\sqrt{\lambda_4} = 31.86$    $\sqrt{\lambda_5} = 45.74$    $\sqrt{\lambda_6} = 61.30$

(a) $c/a = 2/5$



$\sqrt{\lambda_1} = 6.90$    $\sqrt{\lambda_2} = 7.49$    $\sqrt{\lambda_3} = 21.28$    $\sqrt{\lambda_4} = 23.92$    $\sqrt{\lambda_5} = 42.95$    $\sqrt{\lambda_6} = 47.21$
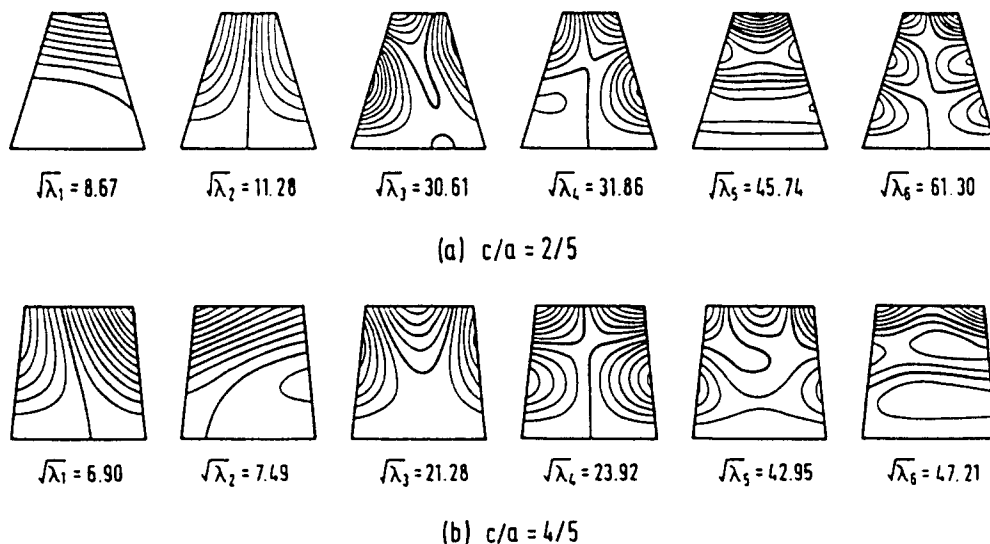
(b) $c/a = 4/5$

Fig. 4. Contour plots for the mode shapes of the sixteen-layer G/E centrally point supported trapezoidal plates $(a/b = 1)$ with stacking sequence of $[(0,45,-45,90)_2]_{sym}$.

Table 5. Convergence patterns of frequency parameters $(\rho\omega^2 a^4 D_0)^{1/2}$ for an eight-layer laminated cantilevered trapezoidal plate $(c/a = 2/5)$ having point supports located at $x = -a/5$, $y = a/2$ and at $x = a/5$, $y = a/2$ (a/b = 1) with a stacking sequence of $[0^\circ, 90^\circ, 90^\circ, 0^\circ]_{sym}$

| | | Mode sequence number | | | | | |
|---|---|---|---|---|---|---|---|
| $S_t$ | Terms | 1 | 2 | 3 | 4 | 5 | 6 |
| 100 | 36 | 12.14 | 15.72 | 33.03 | 40.43 | 42.27 | 52.99 |
| | 40 | 12.14 | 15.72 | 32.98 | 40.03 | 42.27 | 52.85 |
| | 46 | 12.14 | 15.72 | 32.93 | 40.02 | 42.27 | 52.81 |
| | 50 | 12.13 | 15.72 | 32.90 | 40.01 | 42.27 | 52.79 |
| $\infty$ | 36 | 12.19 | 15.78 | 33.40 | 40.58 | 42.56 | 53.22 |
| | 40 | 12.19 | 15.78 | 33.35 | 40.19 | 42.56 | 53.06 |
| | 46 | 12.18 | 15.78 | 33.30 | 40.17 | 42.56 | 53.02 |
| | 50 | 12.18 | 15.78 | 33.27 | 40.16 | 42.56 | 53.00 |

Table 6. Frequency parameters $(\rho\omega^2 a^4 D_0)^{1/2}$ of an eight-layer laminated cantilevered trapezoidal plate (a/b = 1) having elastic point supports located: (i) at $x = -a/5$, $y = a/2$ and at $x = a/5$, $y = a/2$ $(c/a = 2/5)$, or (ii) at $x = -2a/5$, $y = a/2$ and at $x = 2a/5$, $y = a/2$ $(c/a = 4/5)$ with a stacking sequence of $[0^\circ, 90^\circ, 90^\circ, 0^\circ]_{sym}$

| | | Mode sequence number | | | | | |
|---|---|---|---|---|---|---|---|
| $c/a$ | $S_t$ | 1 | 2 | 3 | 4 | 5 | 6 |
| 2/5 | 1 | 8.68 | 12.34 | 21.20 | 30.65 | 38.42 | 49.63 |
| | 10 | 11.69 | 15.22 | 29.80 | 39.22 | 39.81 | 51.52 |
| | 100 | 12.13 | 15.72 | 32.90 | 40.01 | 42.27 | 52.79 |
| | 1000 | 12.18 | 15.78 | 33.24 | 40.15 | 42.53 | 52.98 |
| | 10000 | 12.18 | 15.78 | 33.27 | 40.16 | 42.56 | 53.00 |
| | $\infty$ | 12.19 | 15.78 | 33.27 | 40.16 | 42.56 | 53.00 |
| 4/5 | 1 | 6.45 | 10.40 | 18.15 | 24.37 | 24.46 | 36.76 |
| | 10 | 8.46 | 13.24 | 18.52 | 26.69 | 32.93 | 42.92 |
| | 100 | 8.80 | 13.64 | 18.58 | 27.10 | 35.58 | 44.14 |
| | 1000 | 8.83 | 13.69 | 18.59 | 27.15 | 35.88 | 44.26 |
| | 10000 | 8.84 | 13.69 | 18.59 | 27.15 | 35.91 | 44.27 |
| | $\infty$ | 8.84 | 13.69 | 18.59 | 27.15 | 35.92 | 44.27 |

The first example considered is an eight-ply laminated trapezoidal plate with the stacking sequence of $[0^\circ, 90^\circ, 90^\circ, 0^\circ]_{sym}$. A convergence study for the plate with $a/b = 1$ and $c/a = 2/5$ is carried out and the convergence patterns obtained from the study are given in Table 5. It is observed that for a plate with elastic constant $S_t = 100$ and $\infty$, 50 terms



$\sqrt{\lambda_1} = 12.18$  $\sqrt{\lambda_2} = 15.78$  $\sqrt{\lambda_3} = 33.27$  $\sqrt{\lambda_4} = 40.16$  $\sqrt{\lambda_5} = 42.56$  $\sqrt{\lambda_6} = 53.00$

(a) c/a = 2/5

$\sqrt{\lambda_1} = 8.84$  $\sqrt{\lambda_2} = 13.69$  $\sqrt{\lambda_3} = 18.59$  $\sqrt{\lambda_4} = 27.15$  $\sqrt{\lambda_5} = 35.92$  $\sqrt{\lambda_6} = 44.27$
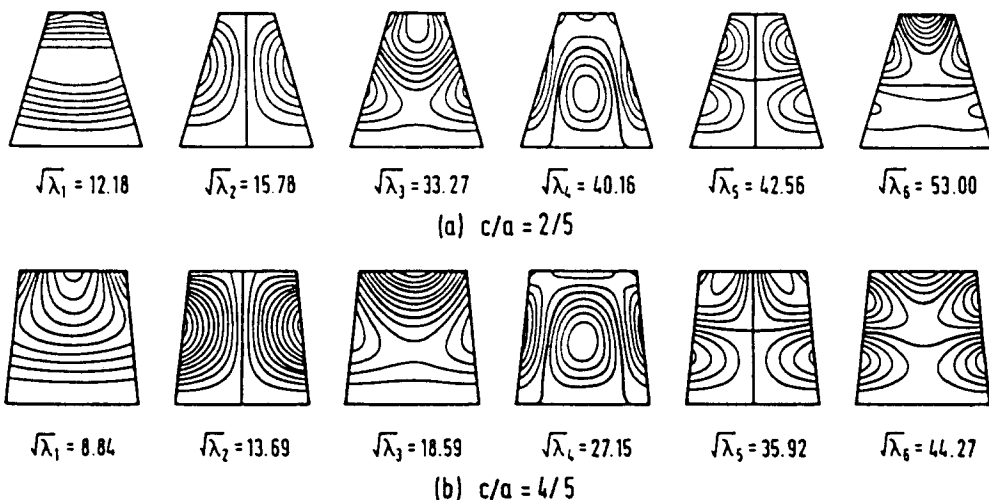
(b) c/a = 4/5

Fig. 5. Contour plots for the mode shapes of the eight-layer G/E points supported trapezoidal plates (a/b = 1) with stacking sequence of $[0^\circ, 90^\circ, 90^\circ, 0^\circ]_{sym}$.

Table 7. Frequency parameters $(\rho h \omega^2 a^4 / D_0)^{1/2}$ of a sixteen-layer laminated cantilevered trapezoidal plate $(a/b = 1)$ having elastic point supports located: (1) at $x = -a/5$, $y = a/2$ and at $x = a/5$, $y = a/2$ $(c/a = 2/5)$, or (ii) at $x = -2a/5$, $y = a/2$ and at $x = 2a/5$, $y = a/2$ $(c/a = 4/5)$ with a stacking sequence of $[(0, 45, -45, 90)_2]_{sym}$

| | | Mode sequence number | | | | | |
|---|---|---|---|---|---|---|---|
| $c/a$ | $S_z$ | 1 | 2 | 3 | 4 | 5 | 6 |
| | 1 | 8.35 | 13.77 | 20.01 | 34.02 | 45.41 | 46.53 |
| | 10 | 11.27 | 17.35 | 29.05 | 42.10 | 45.47 | 51.56 |
| 2/5 | 100 | 11.68 | 18.25 | 32.60 | 45.30 | 45.56 | 55.68 |
| | 1000 | 11.73 | 18.35 | 33.00 | 45.43 | 45.82 | 56.29 |
| | 10000 | 11.73 | 18.37 | 33.04 | 45.43 | 45.85 | 56.35 |
| | $\infty$ | 11.73 | 18.37 | 33.05 | 45.43 | 45.85 | 56.36 |
| | 1 | 6.44 | 11.01 | 17.08 | 26.11 | 27.96 | 46.44 |
| | 10 | 8.96 | 14.72 | 17.81 | 33.25 | 35.43 | 47.27 |
| 4/5 | 100 | 9.43 | 15.40 | 17.99 | 35.94 | 37.86 | 47.63 |
| | 1000 | 9.48 | 15.47 | 18.00 | 36.25 | 38.14 | 47.68 |
| | 10000 | 9.48 | 15.48 | 18.01 | 36.29 | 38.16 | 47.68 |
| | $\infty$ | 9.48 | 15.48 | 18.01 | 36.29 | 38.17 | 47.68 |

are needed to obtain the required convergent results. For this set of problems, it is decided to use 50 terms for all the calculations. An investigation is carried out to study the effect of the spring constant on the vibrational response of the plate. The results obtained from this study are given in Table 6. The study shows that as the spring constant increases to a very large value $(S \geq 10000)$, the plate becomes rigidly supported. The mode shapes obtained for the plate resting on rigid point supports are presented in Fig. 5. The corresponding frequency parameters for each mode shape are also given.

The second example considered is a sixteen-ply laminated trapezoidal plate with the stacking sequence of $[(0, 45, -45, 90)_2]_{sym}$. The effect of the spring constant on the first six frequency parameters for the plates having $c/a = 2/5$ and $4/5$ is studied. The results obtained by using 50 terms are given in Table 7. It is obvious that the spring constants increase with an increase in frequency parameters until $S_z = 1000$, beyond which no significant increase in the frequency parameters is observed. The mode shapes for the rigid points $(S_z \geq 10000)$ supported cantilevered trapezoidal plate having $c/a = 2/5$ and $4/5$ are presented in Fig. 6 together with the corresponding frequency parameters given below each mode.
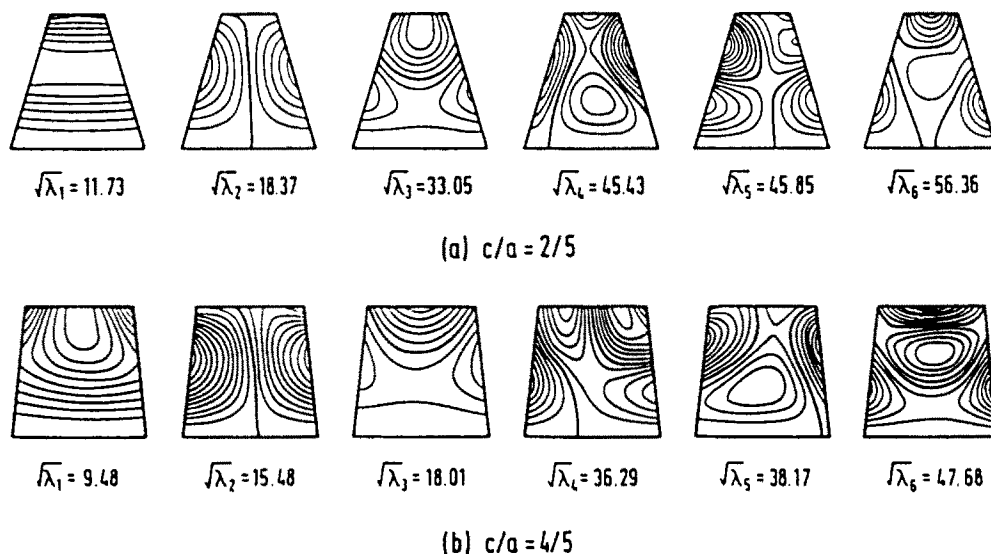


$\sqrt{\lambda_1} = 11.73$  $\sqrt{\lambda_2} = 18.37$  $\sqrt{\lambda_3} = 33.05$  $\sqrt{\lambda_4} = 45.43$  $\sqrt{\lambda_5} = 45.85$  $\sqrt{\lambda_6} = 56.36$

(a) $c/a = 2/5$



$\sqrt{\lambda_1} = 9.48$  $\sqrt{\lambda_2} = 15.48$  $\sqrt{\lambda_3} = 18.01$  $\sqrt{\lambda_4} = 36.29$  $\sqrt{\lambda_5} = 38.17$  $\sqrt{\lambda_6} = 47.68$

(b) $c/a = 4/5$

Fig. 6. Contour plots for the mode shapes of the sixteen-layer G E points supported trapezoidal plates $(a/b = 1)$ with stacking sequence of $[(0, 45, -45, 90)_2]_{sym}$.

## 6. CONCLUSIONS

The proposed sets of 2-D orthogonal polynomials for approximating the deflection shape make the application of the Rayleigh–Ritz method relatively easy to implement for free vibration analysis of symmetrically laminated, points supported, thin trapezoidal composite plates. Several plate problems, results for which are unavailable in the open literature, are solved to show the applicability of the present method. The natural frequencies for the problems are presented for the plates having different fibre orientations, location of points and number of layer in the stacking sequences. The effect of spring constants on the vibrational response for the plates is also investigated.

## REFERENCES

Ashton, J. E. and Anderson, J. D. (1969). The natural modes of vibration of boron epoxy plates. *Shock Vibr. Bull.* **39**, 81–91.

Leissa, A. W. and Narita, Y. (1989). Vibration studies for simply supported symmetrically laminated rectangular plates. *J. Comp. Struct.* **12**, 113–132.

Liew, K. M. and Lam, K. Y. (1990). Application of two-dimensional orthogonal plate functions to flexural vibration of skew plates. *J. Sound Vibr.* **139**, 241–252.

Liew, K. M. and Lam, K. Y. (1991a). A Rayleigh–Ritz approach to transverse vibration of isotropic and anisotropic trapezoidal plates using orthogonal plate functions. *Int. J. Solids Structures* **27**, 189–203.

Liew, K. M. and Lam, K. Y. (1991b). A set of orthogonal plate functions for vibration analysis of regular polygonal plates. *ASME J. Vibr. Acoust.* **113**, 182–186.

Mohan, D. and Kingsbury, H. D. (1971). Free vibrations of general orthotropic plates. *J. Acoust. Soc. Am.* **55**, 998–1002.

Nair, P. S. and Durvasula, S. (1974). Vibration of generally orthotropic skew plates. *J. Acoust. Soc. Am.* **55**, 998–1002.

Srinivasam, R. S. and Ramachandran, S. V. (1975). Vibration of generally orthotropic skew plates. *J. Acoust. Soc. Am.* **57**, 1113–1118.

Whitney, J. M. (1971). Free vibration of anisotropic rectangular plates. *J. Acoust. Soc. Am.* **52**, 448–449.